Supplementary Information

Frontier molecular orbital engineering in spiro-based molecules: achieving aggregation induced delayed fluorescence for non-doped OLEDs

Xue Li[a,b,†], Changshen Shi[c,†], Yuhang Mo[a], Jiancheng Rao[a,b], Lei Zhao[b,], Hongkun Tian[b], Ning Sun[c], Junqiao Ding[a,]**

[a]School of Chemical Science and Technology, Yunnan University, Kunming 650091, P. R. China

[b]State Key Laboratory of Polymer Physics and Chemistry, Changchun Institute of Applied Chemistry, Chinese Academy of Sciences, Changchun 130022, P. R. China

[c]School of Physics and Astronomy, Yunnan University, Kunming 650091, P. R. China

[†]These authors contribute equally to this article.

Corresponding authors: dingjunqiao@ynu.edu.cn; zhaol@ciac.ac.cn

Experimental section

1. Measurements and Characterizations

^{1}H and ^{13}C NMR spectra were recorded with a Bruker Avance NMR spectrometer. MALDI/TOF mass spectra were obtained on an AXIMA CFR MS apparatus (COMPACT). Elemental analyses of carbon, hydrogen, and nitrogen were performed on a Bio-Rad elemental analysis system. Thermal gravimetric analysis (TGA) and differential scanning calorimetry (DSC) were performed on Perkin Elmer-TGA 7 and Perkin Elmer-DSC 7 system under nitrogen at a heating rate of 10 ^{o}C min^{-1}. The UV-Vis absorption and PL spectra were measured by a Perkin-Elmer Lambda 35 UV/vis spectrometer and a Perkin-Elmer LS 50B spectrofluorometer, respectively. For all the tests, the concentration of the solution is 10^{-5} M. The PLQYs were measured using a quartum yield measurement system (C10027, Hamamatsu Photonics) excited at 360 nm. The transient PL spectra were measured by a HORIBA Jobin Yvon Fluorolog-3 spectrofluorometer. Also, the prompt and delayed fluorescence lifetimes were estimated according to a tri-exponential fitting, respectively. Cyclic voltammetry (CV) measurements were obtained in anhydrous dichloromethane with *n*-Bu_4NClO_4 (0.1 mol L^{-1}) as the electrolyte on a CHI660a electrochemical analyzer under a scan rate of 100 mV s^{-1}. A glass carbon electrode, a Ag/AgCl electrode and a Pt wire were used as the working electrode, the reference electrode and the counter electrode, respectively. The HOMO and LUMO energy levels were calculated according to the equation HOMO = $-e[E_{onset,\ ox}$ +4.8] V, LUMO = HOMO + E_g, where $E_{onset,\ ox}$ was the onset value of the first oxidation potential, and E_g was the optical band gap estimated from the PL onset.

The single crystal X-ray diffraction experiments were carried out using a Bruker Smart APEX diffractometer with CCD detector and graphite monochromator, Mo Kα radiation λ = 0.71073 Å. The intensity data were recorded with ω scan mode. Lorentz, polarization factors were made for the intensity data and absorption corrections were performed using SADABS program. The crystal structure was determined using the SHELXTL program and refined using full matrix least squares. All non-hydrogen atoms were assigned with anisotropic displacement parameters, whereas hydrogen atoms were placed at calculated positions theoretically and included in the final cycles of refinement in a riding model along with the attached carbons. Crystallographic data for the structural analyses have been deposited with Cambridge Crystallographic Data Center (CCDC). CCDC reference for AT-spiro-DMACF is 2114927. Copies of this information can be obtained free of charge from The Director, CCDC, 12 Union Road, Cambridge, CB2 1EZ, UK (Fax: +441223336033; E-mail: deposit@ccdc.cam.ac.uk, or http://www.ccdc.cam.ac.uk).

2. Quantum chemical calculations:

All calculations were performed using the Gaussian 09 program package[1]. The geometries in the ground state were directly obtained from the single crystals of TXADO-spiro-DMACF and AT-spiro-DMACF. The vertical excitation energy of $E_{VA}(S_1)$ and $E_{VA}(T_1)$ was calculated at the TDA-PBEα_o/6-31G(d) level using the PCM with cyclohexane solvation according to a semi-empirical descriptor-based optimal Hartree-Fock (OHF) method, the so-called K-OHF method[2].

3. Device fabrication and measurement

The glass substrates precoated with 180 nm ITO with a sheet resistance of 10 Ω/sq were fabricated the devices. First, the ITO substrates were degreased in ultrasonic solvent bath and then dried at 120 °C for 30 min. Before loaded into the vacuum deposition chamber, the ITO surface was treated with UV−ozone for 15 min. Then, 3 nm of HATCN was firstly deposited on the top of ITO substrates, followed by 40 nm TAPC, 10 nm TCTA, 15 nm emitting layer (EML), and 60 nm TmPyPB. As for non-doped device, AT-spiro-DMACF is used as the EML independently. As for doped devices, AT-spiro-DMACF is dispersed in mCP with different concentration. Finally, 1 nm of LiF and 120 nm of Al were sequentially deposited to form the cathode. All the layers were grown by thermal evaporation in a high-vacuum system with a pressure less than 5×10^{-4} Pa without breaking vacuum. The organic materials were evaporated at the rate in a range of 1−2 Å/s, and the metal Al was evaporated at the rate of 8−10 Å/s. The overlap between ITO and Al electrodes was 4 mm × 4 mm, which is the active emissive area of the OLED devices. The EL spectra and CIE coordinates were measured using a PR650 spectra colorimeter. The current−voltage and brightness−voltage curves of devices were measured using a Keithley 2400/2000 source meter and a calibrated silicon photodiode. The EQE was calculated from the luminance, current density and EL spectra assuming a Lambertian distribution. All the measurements were carried out at room temperature under ambient conditions.

3. Synthesis

All solvents for chemical synthesis were refined according to the standard procedures. 4,4'-dibromo-2-iodo-1,1'-biphenyl were prepared according to literature methods[3].

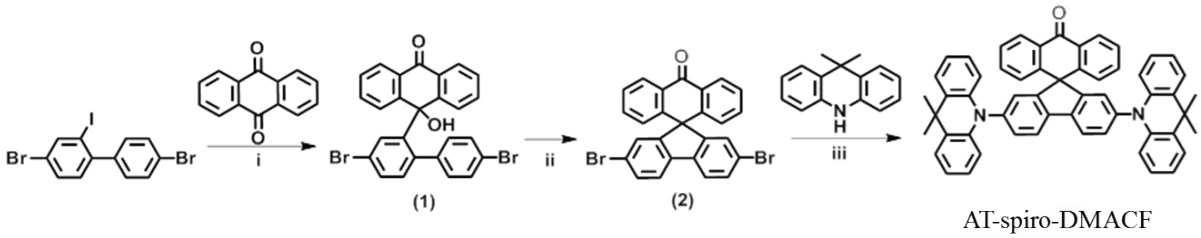

Scheme S1. Synthetic Route for AT-spiro-DMACF. Reagents and conditions: (i) Mg, I_2, LiCl, CH_3CH_2Br, THF, 60 °C; (ii) CH_3COOH, 1,4-Dioxane, HCl, H_2O, 100 °C; (iii) $Pd_2(dba)_3$, P(*t*-Bu)$_3$HBF$_4$, *t*-BuONa, trimethylbenzene, 135 °C.

10-(4,4'-dibromo-[1,1'-biphenyl]-2-yl)-10-hydroxyanthracen-9(10H)-one (**1**): All the glass containers were heated by a heating gun and cooled to room temperature for 3 times and the reaction was conducted under argon atmosphere. A mixture of ~1 g LiCl, 1 iodine grain, ~1 g magnesium pieces were added before ~100 mL dry THF. A solution of 4,4'-Dibromo-2-iodo-1,1'-biphenyl (6.54 g, 15 mmol) and 1 drop of bromoethane (as the initiator) in ~50 mL of dry THF was added dropwise into the system. After being stirring for 30 min at 60 °C, the solution was transfer into a flask with anthracene-9,10-dione (4.06 g, 19.5mmol) through a needle tube connecting the two spaces, stirred at 60 °C for 2 h. The mixture was cooled to room temperature before ~200 mL of water was added, extracted with 200 mL of dichloromethane twice. The combined organic solution was dried with Na_2SO_4, filtrated, and removed the solvent in vacuum. The residue was not further purified by column

chromatography on silica gel with hexane/dichloromethane (1:5) as eluent to give a white solid **1** (4.91 g, 63%). ^{1}H NMR (400 MHz, $CDCl_3$) δ 8.22 – 8.09 (m, 2H), 7.52 – 7.44 (m, 2H), 7.43 – 7.36 (m, 3H), 7.34 (d, J = 1.7 Hz, 1H), 6.96 – 6.82 (m, 5H), 6.22 – 6.07 (m, 2H), 1.55 (s, 1H).

2',7'-dibromo-10H-spiro[anthracene-9,9'-fluoren]-10-one (**2**): A mixture of **1** (4.25 g, 8.17 mmol), 1,4-Dioxane (100 mL) and acetic acid (300 mL) was heated to 100 °C (colorless transparent solution). 20 mL of hydrochloric acid (6 mol/L) was added slowly. After being stirring overnight, the system was cooled to room temperature resulting in some slightly yellow precipitation. The solid was collected by filtration and washed with water three times, and dried in vacuum at 70 °C overnight. The crude product was further purified by column chromatography on silica gel with hexane/dichloromethane (1:1) as eluent to give a white solid **2** (3.05 g, 74%). ^{1}H NMR (400 MHz, $CDCl_3$) δ 8.44 (dd, *J* = 7.9, 1.3 Hz, 2H), 7.70 (d, *J* = 8.2 Hz, 2H), 7.53 (dd, *J* = 8.2, 1.8 Hz, 2H), 7.44 (td, *J* = 7.7, 1.2 Hz, 2H), 7.37 – 7.30 (m, 2H), 6.98 (d, *J* = 1.7 Hz, 2H), 6.54 (dd, *J* = 8.0, 0.7 Hz, 2H).

AT-spiro-DMACF: The reaction was conducted under an argon atmosphere. A mixture of **2** (1.10 g, 2.20 mmol), 9,9-dimethyl-9,10-dihydroacridine (1.10 g, 5.30mmol), $Pd_2(dba)_3$ (0.050 g, 0.053 mmol), $P(t\text{-}Bu)_3HBF_4$ (0.064 g, 0.22 mmol) and t-BuONa (2.10 g, 22 mmol) was added before ~50 mL trimethylbenzene and heated to 135 °C overnight. The system was cooled to room temperature and most of the solvent was removed by reduced pressure distillation. The residue was further purified by column chromatography to give a light yellow solid AT-spiro-DMACF (1.42 g, 85%). Then, the product was recrystallized in a

mixed solvent of dichloromethane and n-hexane twice. ^{1}H NMR (400 MHz, $CDCl_3$) δ 8.33 (dd, *J* = 7.5, 1.7 Hz, 2H), 8.18 (d, *J* = 8.0 Hz, 2H), 7.43 – 7.37 (m, 10H), 6.86 – 6.90 (m, 12H), 6.11 (m, 4H), 1.60 (s, 12H). ^{13}C NMR (126 MHz, $CDCl_3$) δ 183.48, 156.24, 143.39, 141.75, 140.62, 140.11, 128.58, 127.92, 127.58, 126.25, 125.34, 120.68, 113.66, 58.17, 35.91, 31.34. MS (MALDI-TOF) m/z: 758.3 [M^+] . Anal.Calcd. for $C_{56}H_{42}N_2O$: C, 88.62; H, 5.58; N, 3.69. Found: C, 88.67; H, 5.59; N, 3.62.

References:

1. M. J. Frisch, G. W. Trucks, H. B. Schlegel, et al., Gaussian, Inc., Wallingford CT, 2013.

2. C. Wang, C. Deng, D. Wang, Q. Zhang, *J. Phys. Chem. C* 2018, **122**, 7816.

3. J. C. Rao, C. Y. Zhao, Y. P. Wang, K. Y. Bai, S. M. Wang, J. Q. Ding, L. X. Wang, *ACS Omega,* 2019, **4**, 1861-1867.

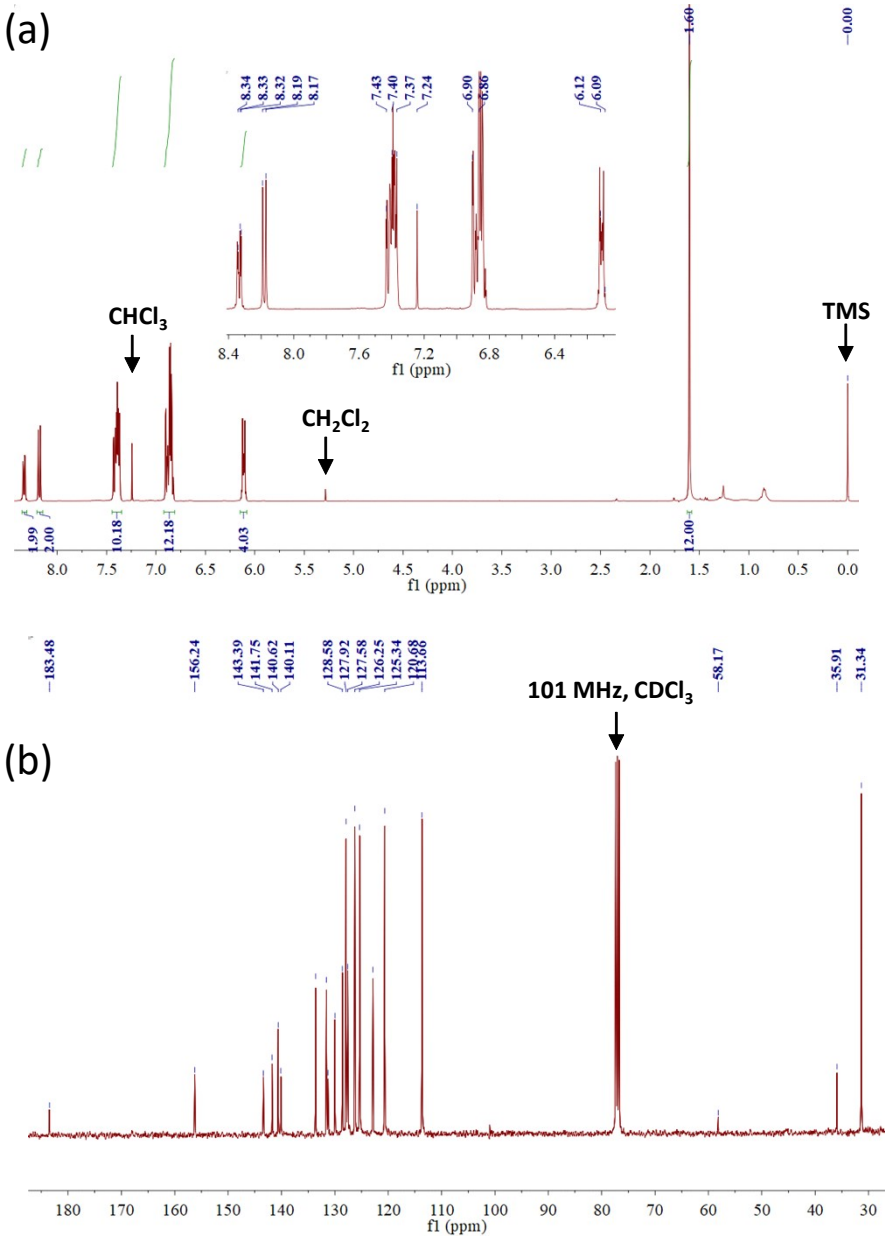

Figure S1. ^{1}H NMR (a) and ^{13}C NMR (b) spectra for the final product AT-spiro-DMACF.

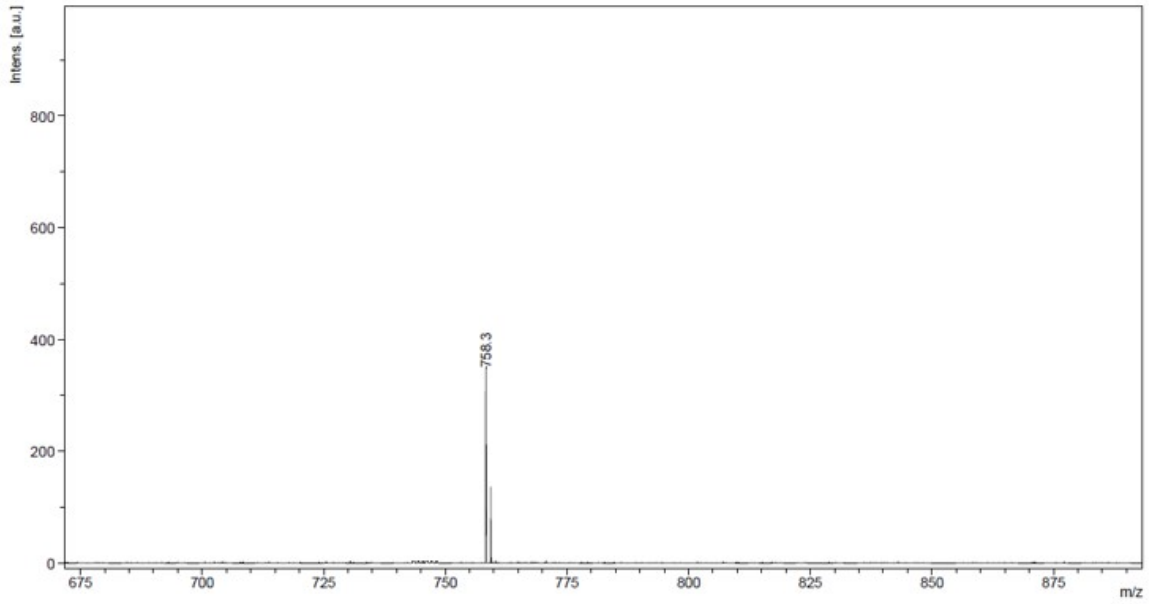

Figure S2. MALDI-TOF mass spectrum of the final product AT-spiro-DMACF.

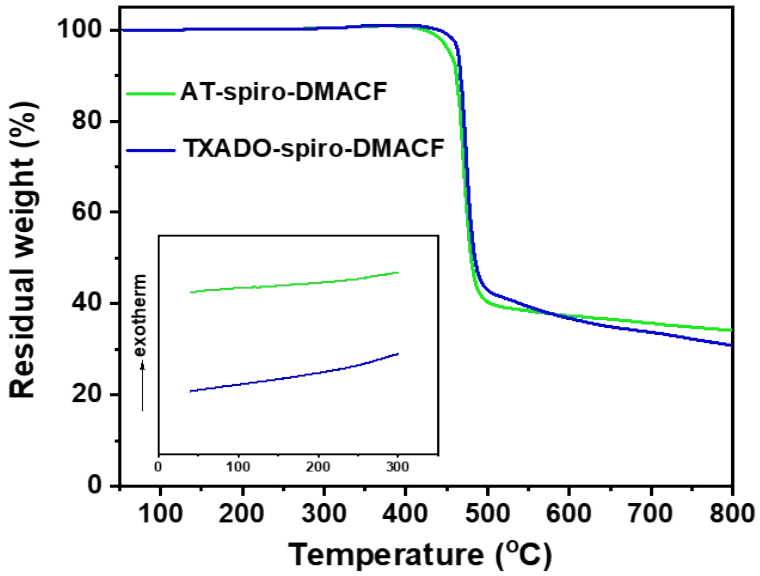

Figure S3. Comparison of the TGA and DSC curves (inset) under nitrogen atmosphere between AT-spiro-DMACF and TXADO-spiro-DMACF.

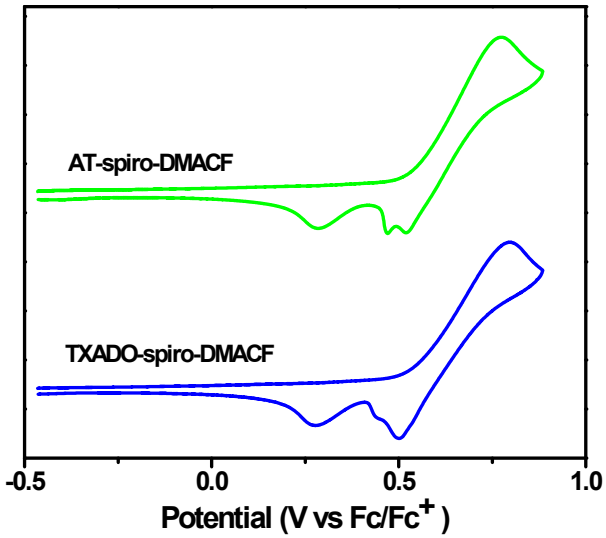

Figure S4. Comparison of the cyclic voltammetry in dichloromethane solution between AT-spiro-DMACF and TXADO-spiro-DMACF.

Table S1. X-ray crystallographic data of TXADO-spiro-DMACF and AT-spiro-DMACF.

Name	TXADO-spiro-DMACF	AT-spiro-DMACF
Empirical formula	C55H42N2O2S	C56H42N2O
Formula weight	794.97	758.92
Temperature	188(2)	293(2)
Crystal system	monoclinic	triclinic
Space group	C c	P-1
Unit cell dimensions	a = 23.7490(11) Å b = 31.2851(15) Å c = 17.9917(9) Å alpha=90 deg beta=108.379(2) deg gamma=90 deg	a = 10.2046(15) Å b = 12.2649(19) Å c = 18.468(3) Å alpha = 70.616(3) deg beta = 88.890(4) deg gamma = 68.710(3) deg
Volume	12685.8(11)	2018.1(5)
Z	12	2
Density	1.249	1.249
F(000)	5016	800
Radiation	Mo Kα radiation (λ = 0.71073 Å)	Mo Kα radiation (λ = 0.71073 Å)
Cell measurement theta min	2.1518	2.3347
Cell measurement theta max	21.8399	18.9287
CCDC	1880025	2114927

Table S2. Calculated data in toluene for TXADO-spiro-DMACF and AT-spiro-DMACF.

Compound	α_0	$E_{VA}(S_1)$ [eV]	$E_{VA}(T_1)$ [eV]	ΔE_{ST} [eV]	f (S_1)
TXADO-spiro-DMACF	0.3484	3.4103	3.1133	0.2970	0.0214
AT-spiro-DMACF	0.3068	3.1275	3.1106	0.0169	0.0016

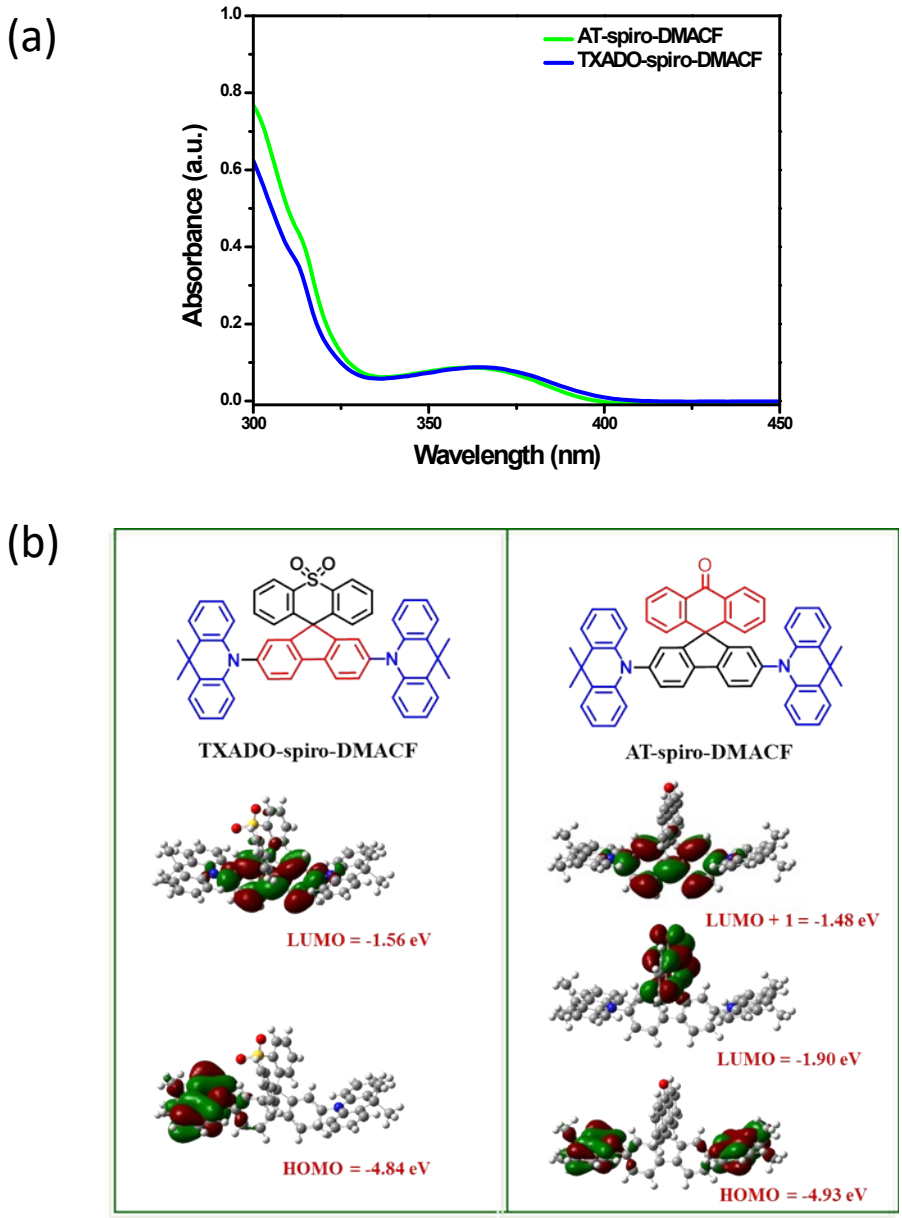

Figure S5. Comparison of UV-Vis absorption spectra in toluene between AT-spiro-DMACF and TXADO-spiro-DMACF (a), and their frontier molecular orbital distributions (b).

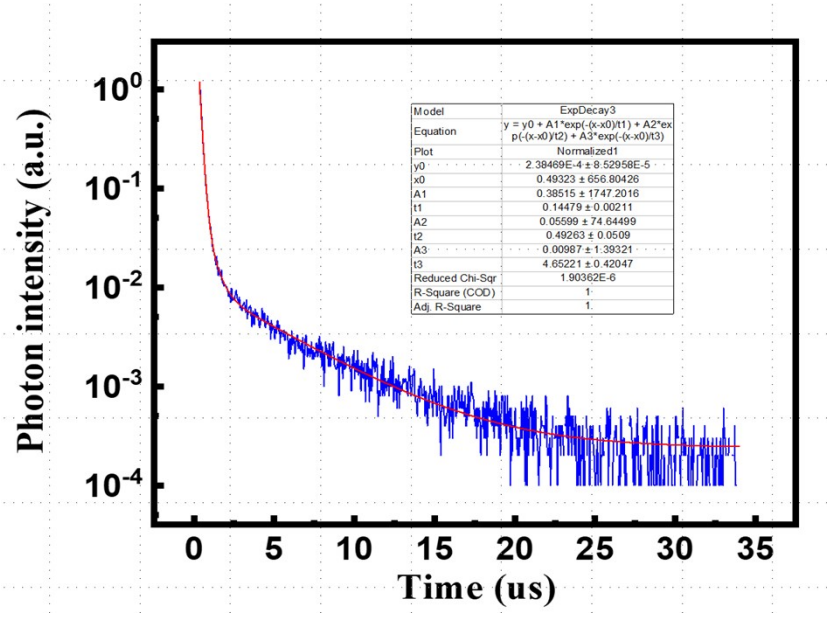

Figure S6. The transient PL spectrum of AT-spiro-DMACF in neat film, which is fitted by a tri-exponential decay.

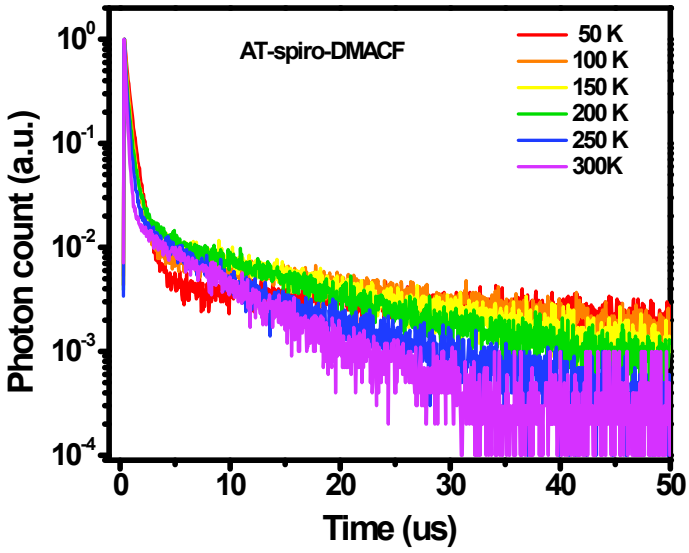

Figure S7. The temperature-dependent transient PL spectra of AT-spiro-DMACF in neat film.

(a)

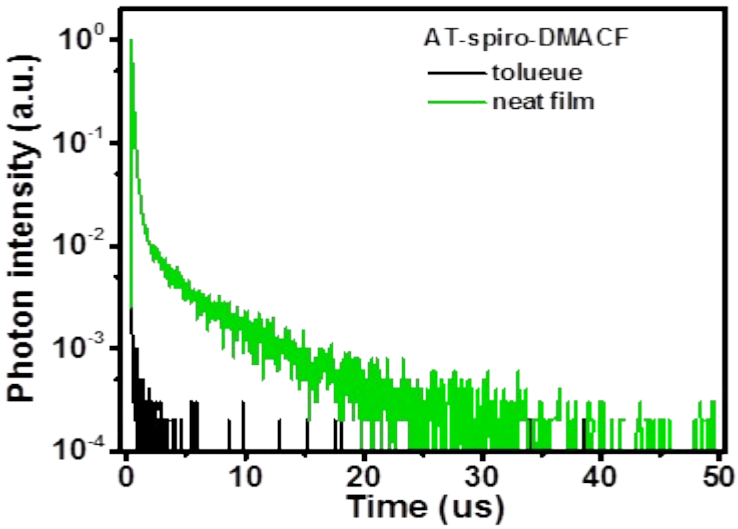

(b)

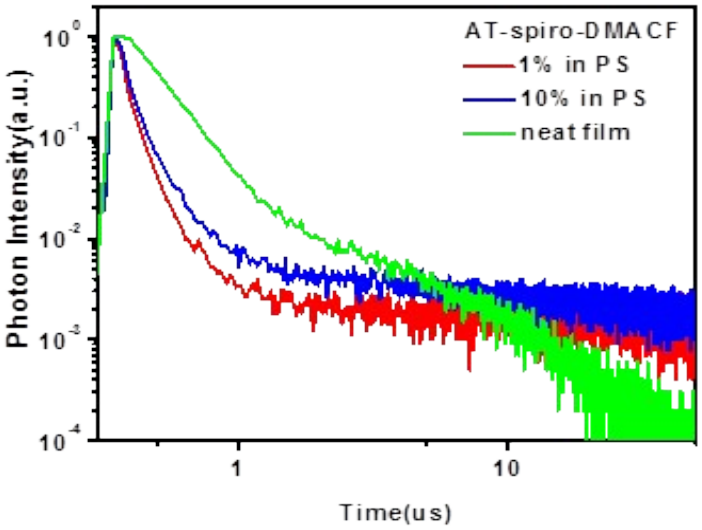

Figure S8. (a) Comparison of the transient PL spectra between toluene and neat film; (b) PL decay for doped films of AT-spiro-DMACF in PS with varied concentration.

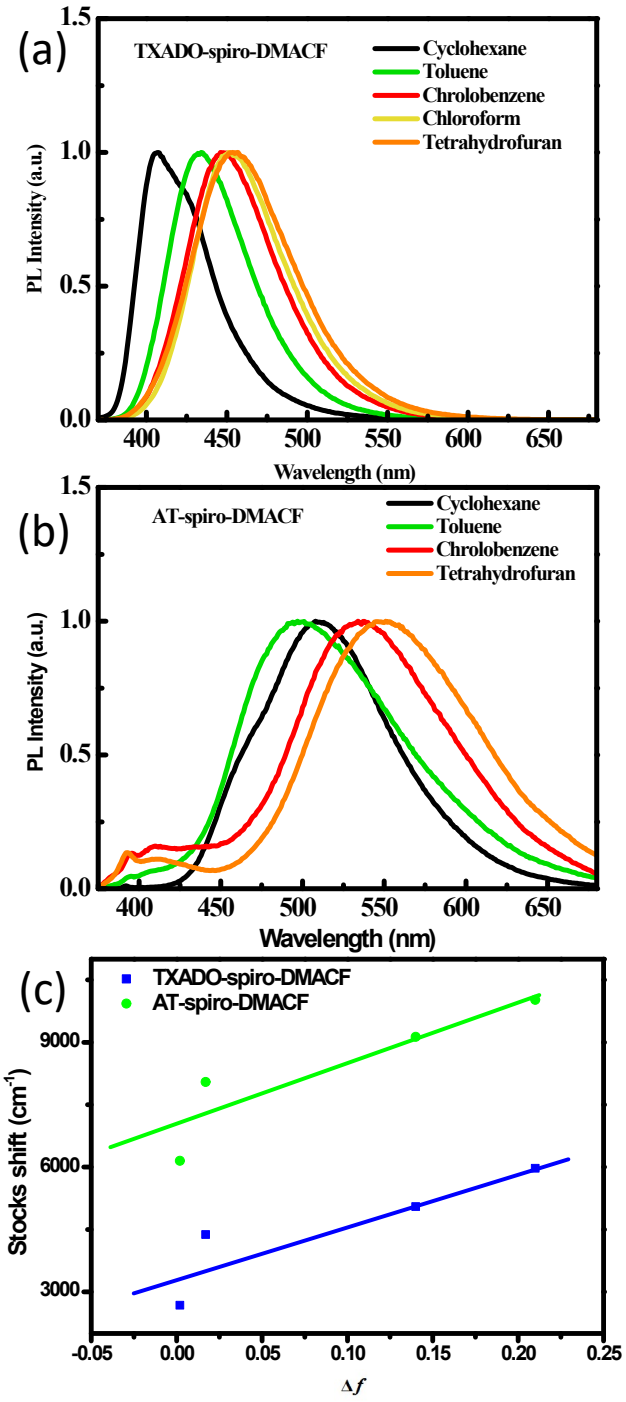

Figure S9. PL spectra in different polarity solvents for TXADO-spiro-DMACF (a) and AT-spiro-DMACF (b), and the linear correlation of the solvent orientation polarization (Δf) with the Stokes shift (c).

Table S3. Related data for Figure S9c.

solvent	*Δf*	TXADO-spiro-DMACF			AT-spiro-DMACF		
		$\lambda_{abs,\ max}$ (nm)	$\lambda_{em,\ max}$ (nm)	Stokes shift (cm^{-1})	$\lambda_{abs,\ max}$ (nm)	$\lambda_{em,\ max}$ (nm)	Stokes shift (cm^{-1})
Cyclohexane	0.0019	367	407	2678	367	474	6151
Toluene	0.017	364	437	4589	355	497	8049
Chlorobenzene	0.14	364	446	5051	359	534	9129
Tetrahydrofuran	0.21	359	457	5973	355	551	10020

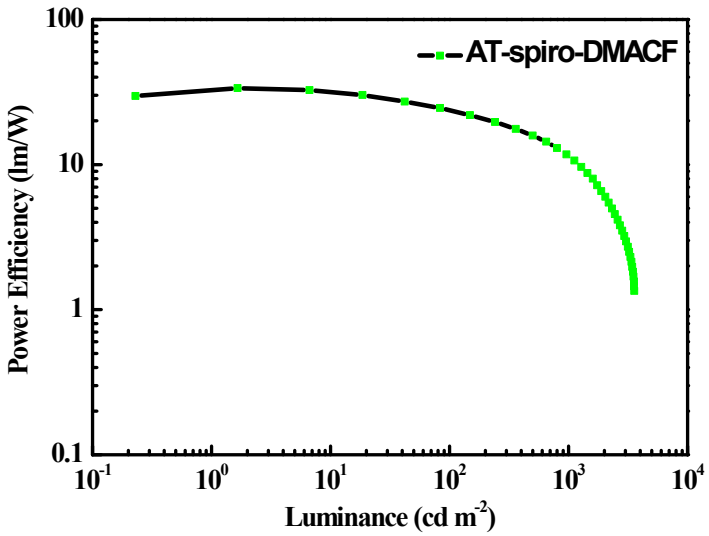

Figure S10. Power efficiency as a function of luminance for the non-doped device of AT-spiro-DMACF.

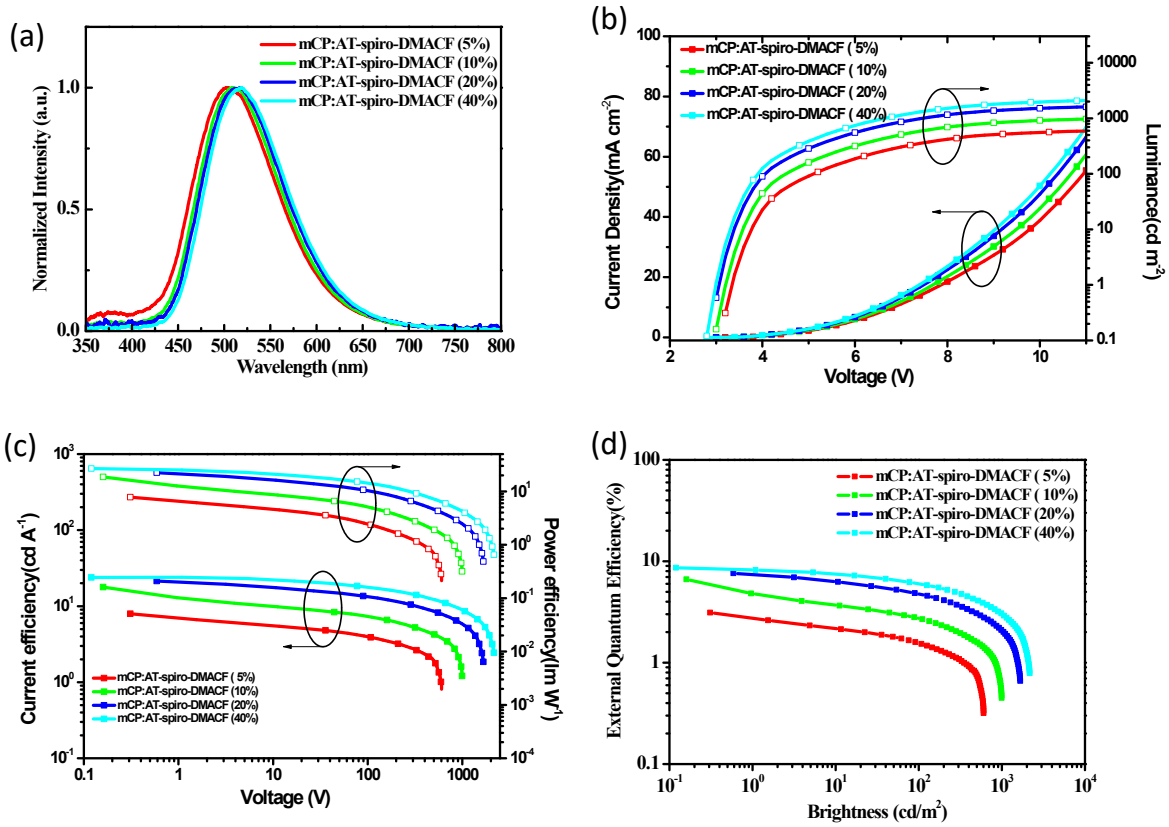

Figure S11. Doped device performance for TXADO-spiro-DMACF in mCP: (a) EL spectra at a driving voltage of 5.0 V; (b) Current density-voltage-luminance characteristics; (c) Current efficiency and power efficiency as the function of luminance; (d) EQE as the function of luminance.

Table S4. Doped and non-doped device performance for TXADO-spiro-DMACF.

Doping Concentration	V_{on} [a] (V)	L_{max} (cd/m^2)	CE [b] (cd/A)	PE [b] (lm/W)	EQE [b] (%)	λ_{EL} [c] (nm)	CIE [d] (x,y)
5 wt.%	3.4	602	7.92	7.78	3.1	504	(0.24, 0.42)
10 wt.%	3.2	994	12.93	12.69	4.8	509	(0.25, 0.45)
20 wt.%	3.2	1666	21.4	22.4	7.6	513	(0.27, 0.48)
40 wt.%	3.0	2166	23.9	26.8	8.6	519	(0.28, 0.50)
100 wt.% (Non-doped)	2.8	3565	31.1	33.7	9.8	532	(0.35, 0.54)

[a]Turn-on voltage at 1 cd/m^2; [b]Maximum data; [c]Maximum EL wavelength; [d]CIE coordinates at 5V.